Strain-induced gap modication of two two-dimensional carbon phosphide compoud semiconductor materials

Xi Fu[1,2*], Yuanping Chen[2]

Abstract. We characterized the electronic structure of two-dimensional carbon phosphide compoud semiconductor materials predicted by particle swarm optimization methodology using first principles calculations based on density functional theory. We focused on the role of strain on the band structure of the two-dimensional materials. We find that under a tensile strain on the range of -5% to 5%, the band gap of C_2P_4-1 (P-42_1m symmetry) indicating a linear relationship with the strain ratio, and the band gap of C_2P_4-2 (P-1 symmetry) decreases accordingly with different strains. These results indicate that strain is a powerful avenue to modulate their properties, especially the band gap of C_2P_4-1 can be tuned larger than 2.0 eV which expands their potential applications in optoelectronics.

Key words. Electronic Structure, Carbon Phosphide Compound, Tensile Strain.

1. Introduction

Two dimensional (2D) materials, such as graphene, MoS_2 and black phosphorus, have attracted intensive interset recently owing to their novel electronic properties that differ from their bulk counterparts.[1-3] For example, MoS2 monolayer has a direct bandgap of 1.8-1.9 eV while the MoS2 has an indirect bandgap about 1.5 eV.[4] Among various two-dimensional (2D) materials, tunable electronic properties are crucial for their applications in optoelectroncis.[4] To achieve tunable bandgaps for 2D materials, two widely used engineering stategies are the application of either an external electric field or a tensile strain.[4] Therefore, in this paper we will study the influences of tensile strain on two 2D structures.

Whether 2D monolayer between Carbon and Phosphorus elements exists has been considered. A survey of experimental literature show that amorphous Carbon Phosphide (CP) films can be synthesized using radio frequency plasma deposition and pulsed laser deposition, for which the ratios of P/C in the films are widely con-

---

[1]College of Science, Hunan Universtiy of Science and Engineering, Yongzhou, 425199

[2]School of Physics and Optoelectronics, Xiangtan University, Xiangtan, 411105

trolled via the ratios of PH_3/PH_4 gas.[5-8] Tan et al. reported the synthesis of a high-performance composite few-layer b-PC field-effect transistor which achieved a high mobility at room temperature via a novel carbon doping technique.[9] Wang et al. recently predicted three different geometrical phases of CP monolayers based on the Particle Swarm Optimization (PSO) method and density functional theory. Among those structures, two phases α-CP and β-CP are semiconducts with superior carrier mobility, while another phase γ-CP exhibits a semi-metallic behavior with Dirac cones.[10] Very recently, Rajbanshi et al. reported that the co-existence of nonbonding electron with metallic properties for β_0-PC was explained on the basis of electron delocalization involving P and C atoms along zigzag chain of β_0-PC. [11] In this paper, we will focus on two Two-Dimensional Carbon Phosphide Compouds C_2P_4-1 and C_2P_4-2 which have been predicted by particle swarm optimization methodology, and study the strain-induced gap modication of two structures.

2. Computational methods

We use the Perdew-Burke-Ernzerhof (PBE) exchange-correlation of the generalized gradient approximation (GGA)[12–14] as realized in the VASP package to Underly ab initio structural relaxations and electric properties. [15, 16] The energy cutoff is 450 eV and the Brillouin zone is sampled using k-points with 0.02 $^{-1}$ spacing in the Monkhorst-Pack scheme. Structural optimization was executed until the enthalpy change per atom was less than 1×10^{-6} eV, and the forces on atoms were taken as 0.001 eV/Å.

We focus on the implications of in-plane biaxial and uniaxial tensile strains, and the strain ratio is defined as

$$S_a = \Delta a/a \times 100\%\,, \tag{1}$$

and

$$S_b = \Delta b/b \times 100\%\,, \tag{2}$$

with unstrained cell parameters a and b, strained cell parameters $\Delta a + a$ and $\Delta b + b$. The biaxial tensile strains change the two parameters simultaneously. For the uniaxial tensile strains, when changing the a directional cell parameter, one should do structural optimization in order to acqurie the best structrue and the bese another cell parameter.

3. Results and discussion

Figure 1 indicates two structures of carbon phosphide compounds, as well as the carbon atoms are labeled by little spheres and the phosphide atoms are label by large spheres. In the 2D structure C_2P_4-1, each phosphorus atom is bonded with two carbon atoms and one phosphorus atom indicating sp^3 hybridization, and each carbon atom is bonded with four phosphorus atoms implying the carbon atoms are sp3 hybridized. In the 2D structure C_2P_4-2, each carbon atom is bonded with three

nearest neighbors in a planar shape, implying the carbon atoms are sp^2 hybridized, and each phosphorus atom is bonded with three neighboring atoms in a buckled shape, indicating sp^3 hybridization of phosphorus atoms.
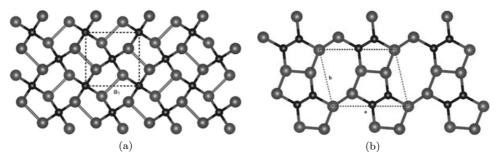

(a)   (b)

Fig. 1. The structures of two carbon phosphide compounds: (a) C_2P_4-1 (space group, P-42_1m (113)) and (b) C_2P_4-2 (space group, P-1(2)).

Table 1. The structural parameters two 2D structures

C_2P_4-1	$a(\text{Å})$	$b(\text{Å})$	$\alpha(°)$	$\beta(°)$	$\gamma(°)$
	4.1423	4.1423	90	90	90
C_2P_4-2	$a(\text{Å})$	$b(\text{Å})$	$\alpha(°)$	$\beta(°)$	$\gamma(°)$
	5.680	4.381	90	90	103.723

Corresponding lattice parameters including the cell parameters and bond angles of C_2P_4-1 and C_2P_4-2 are shown in table 1. From the table, one can find that the structure C_2P_4-1 has the same cell parameters $a = b = 4.1423$ Å, so for its uniaxial tensile strains we only need calculate one direction strain and along a or b direction the influences of uniaxial tensile strain are equal. For the structure C_2P_4-2 the cell parameters $a = 5.680$ Å and $b = 4.381$ Å, then we should discuss the influences of two uniaxial tensile strains respectively.

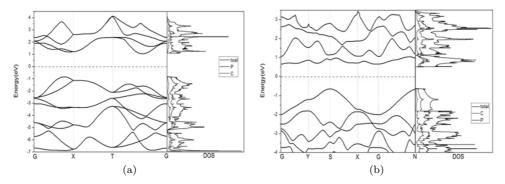(a)   (b)

Fig. 2. Band structure and density of states of (a) C_2P_4-1 and (b) C_2P_4-2.

The calculated band structures and density of states (DOS) in Figure 2 indicate that C_2P_4-1 and C_2P_4-2 are semiconductors with an indirect band gap of 1.89 eV

and 1.30 eV at the GGA-PBE level of theory, respectively. The structure C_2P_4-1 has an wider band gap, which may create a method for transistors, optoelectronic devices and mechanical sensors.[17] Moreover, our calculations find that only the d orbital of carbon and phosphorus atoms contribute to the DOS, as well as DOS strength of phosphorus atoms are larger than that of carbon atoms.
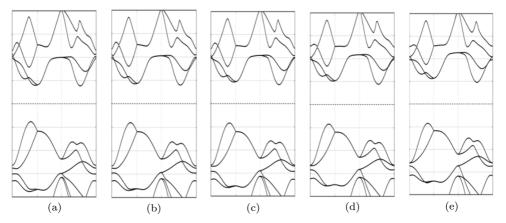

Fig. 3. Band structures of C_2P_4-1 with different biaxial tensile strain ratios (a) $S_a = S_b = -5\%$, (b) $S_a = S_b = -4\%$, (c) $S_a = S_b = -3\%$, (d) $S_a = S_b = -2\%$ and (e) $S_a = S_b = -1\%$ when compressing the cell parameters.

Now we start to discuss the influences of tensile strain to the band structures of two materials. C_2P_4-1 cell is square with the same cell parameters and we only consider a direction uniaxial strain, however, C_2P_4-2 cell is parallelogram with different cell parameters and two direction should be considered.[4,18] Figure 3 and Figure 4 show different band structures of C_2P_4-1 for different biaxial strain ratios, as well as the K-points path is G-X-T-G and the longitudinal energy range is -4 eV to 4 eV. One can find that in Fig.3 when compressing the cell parameter a and b along two directions ($a = b$ for C_2P_4-1) from $S_a = S_b = -5\%$ ($\Delta a + a = \Delta b + b = 3.9352$ Å) to $S_a = S_b = -1\%$ ($\Delta a + a = \Delta b + b = 4.1009$ Å), the value of each band gap increases accordingly. Moreover in Fig.4 when stretching the cell parameter a and b along two directions ($a = b$ for C_2P_4-1) from $S_a = S_b = 1\%$ ($\Delta a + a = \Delta b + b = 4.1837$ Å) to $S_a = S_b = 5\%$ ($\Delta a + a = \Delta b + b = 4.34942$ Å), the value of each band gap also increases respectively. These results present that the tensile strain is indeed a good way of modulating the bandgap of the semiconductor structure C_2P_4-1.

Figure 5 and Figure 6 show the influences of uniaxial tensile strains to the band structures of C_2P_4-1. We fixed the cell parameter $\Delta a + a$ along one direction to the needed strain ratios and acquired the best structure by doing structural optimization, therefore, calculated the eneryg band of structure. Due the symmetry of C_2P_4-1, we only discuss the influences along one cell direction. In Fig.5, when the ratio changes from $S_a = -5\%$ ($\Delta a + a = 3.9352$ Å) to $S_a = -1\%$ ($\Delta a + a = 4.1009$ Å), the value of each band gap increases accordingly which is consistent with the results for the case of biaxial tensile strain. In Fig.6, when the ratio changes from $S_a = 1\%$ ($\Delta a + a = 4.1837$ Å) to $S_a = 5\%$ ($\Delta a + a = 4.34942$ Å), the value of each band
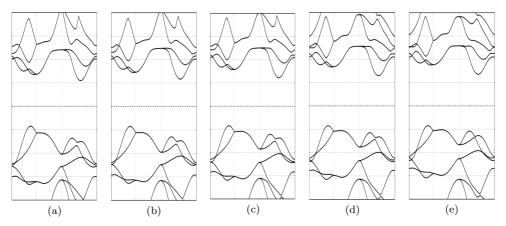
Fig. 4. Band structures of C_2P_4-1 with different biaxial tensile strain ratios (a) $S_a = S_b = 1\%$, (b) $S_a = S_b = 2\%$, (c) $S_a = S_b = 3\%$, (d) $S_a = S_b = 4\%$ and (e) $S_a = S_b = 5\%$ when stretching the cell parameters.
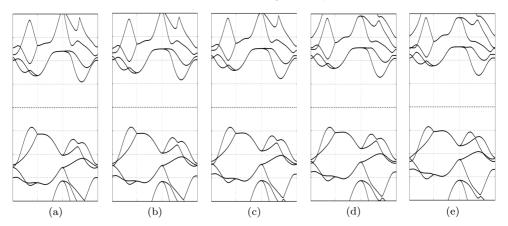

Fig. 5. Band structures of C_2P_4-1 with different uniaxial tensile strain ratios (a) $S_a = -5\%$, (b) $S_a = -4\%$, (c) $S_a = -3\%$, (d) $S_a = -2\%$ and (e) $S_a = -1\%$ when compressing the cell parameters.

gap also increases which is also consistent with the results for the case of biaxial tensile strain. Moreover, one can find that the increaseing of band gap is linear to the tensile strain ratio, and we can image that when the tensile strain ratio reaches larger values, the band gap will also become higher, such as than 2.0 eV, and may be useful in the application of large-gap optoelectronic devices.[17]

Figure 7 and Figure 8 show different band structures of C_2P_4-2 for different biaxial strain ratios, as well as the K-points path is G-Y-S-X-G-N and the longitudinal energy range is -4 eV to 4 eV. One can find that in Fig.7 when compressing the cell parameter a and b along two directions from $S_a = S_b = -5\%$ ($\Delta a + a = 5.396$ Å, $\Delta b + b = 4.162$ Å) to $S_a = S_b = -1\%$ ($\Delta a + a = 5.6232$ Å, $\Delta b + b = 4.337$ Å), the value of each band gap decreases accordingly. Moreover in Fig.4 when stretching the cell parameter a and b along two directions from $S_a = S_b = 1\%$ ($\Delta a + a = 5.737$
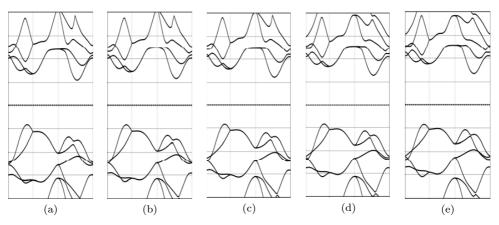
Fig. 6. Band structures of C_2P_4-1 with different uniaxial tensile strain ratios (a) $S_a = 1\%$, (b) $S_a = 2\%$, (c) $S_a = 3\%$, (d) $S_a = 4\%$ and (e) $S_a = 5\%$ when stretching the cell parameters.
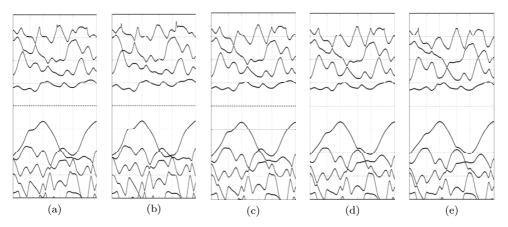

Fig. 7. Band structures of C_2P_4-2 with different biaxial tensile strain ratios (a) $S_a = S_b = -5\%$, (b) $S_a = S_b = -4\%$, (c) $S_a = S_b = -3\%$, (d) $S_a = S_b = -2\%$ and (e) $S_a = S_b = -1\%$ when compressing the cell parameters.

Å, $\Delta b + b = 4.425$ Å) to $S_a = S_b = 5\%$ (($\Delta a + a = 5.964$ Å, $\Delta b + b = 4.600$ Å), the value of each band gap also decreases respectively. These results also show that the change of tensile strain can modulate the bandgap of the semiconductor structure C_2P_4-2 which present different results with those for the structure semiconductor C_2P_4-1. Furthermore, with the strain ratios increasing, two structures remain indirect semiconductors and no indirect-to-direct transition found.

Figure 9 - Figure 12 show the influences of uniaxial tensile strains along two different direction to the band structures of C_2P_4-2. In Fig.9 and Fig.10, the cell parameter $\Delta a + a$ is fixed, and In Fig.11 and Fig.12, the cell parameter $\Delta b + b$ is fixed. In Fig.9 when the ratio changes from $S_a = -5\%$ ($\Delta a + a = 5.396$ Å) to $S_a = -1\%$ ($\Delta a + a = 5.6232$ Å), in Fig.10 when the ratio changes from $S_a = 1\%$ ($\Delta a + a = 5.7396$ Å) to $S_a = 5\%$ ($\Delta a + a = 5.964$ Å), In Fig.11 when the ratio
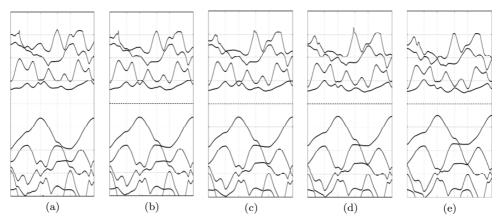
Fig. 8. Band structures of C_2P_4-2 with different biaxial tensile strain ratios (a) $S_a = S_b = 1\%$, (b) $S_a = S_b = 2\%$, (c) $S_a = S_b = 3\%$, (d) $S_a = S_b = 4\%$ and (e) $S_a = S_b = 5\%$ when stretching the cell parameters.
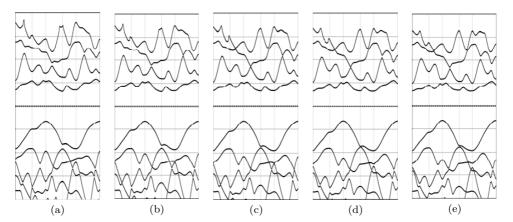

Fig. 9. Band structures of C_2P_4-2 with different uniaxial tensile strain ratios (a) $S_a = -5\%$, (b) $S_a = -4\%$, (c) $S_a = -3\%$, (d) $S_a = -2\%$ and (e) $S_a = -1\%$ along the cell parameter a when compressing the cell parameters.

changes from $S_b = -5\%$ ($\Delta b + b = 4.162$ Å) to $S_b = -1\%$ ($\Delta b + b = 4.3372$ Å), and in Fig.11 when the ratio changes from $S_b = 1\%$ ($\Delta b + b = 4.425$ Å) to $S_b = 5\%$ ($\Delta b + b = 4.600$ Å), the value of each band gap decreases respectively which is consistent with the results for the case of biaxial tensile strain, indicating that the energy gap of C_2P_4-2 can be modulated by the tensile strain.

Figure 13 shows how two structures C_2P_4-1 and C_2P_4-2 transfer from semiconductors to metals when we further altered the biaxial strain ratio of the structures. For the C_2P_4-1, it will change to the metal when the ratio decreases to a lower strain ratio as about -18%, while for the C_2P_4-2 it will turn into the metal when the ratio increases to a higher strain ratio as to about 20%.
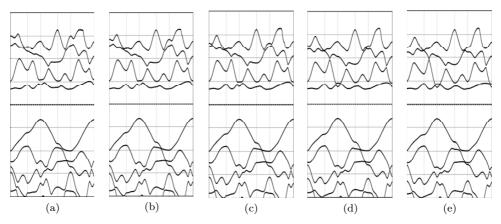
Fig. 10. Band structures of C_2P_4-2 with different uniaxial tensile strain ratios (a) $S_a = 1\%$, (b) $S_a = 2\%$, (c) $S_a = 3\%$, (d) $S_a = 4\%$ and (e) $S_a = 5\%$ along the cell parameter a when stretching the cell parameters.
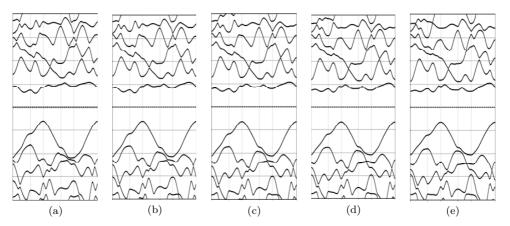

Fig. 11. Band structures of C_2P_4-2 with different uniaxial tensile strain ratios (a) $S_b = -5\%$, (b) $S_b = -4\%$, (c) $S_b = -3\%$, (d) $S_b = -2\%$ and (e) $S_b = -1\%$ along the cell parameter b when compressing the cell parameters.

4. Conclusion

In conclusion, we have studied the influences of tensile strain on the band structure of the two-dimensional carbon phosphide compoud semiconductor materials using first principles calculations based on density functional theory. We have found that under a tensile strain on the range of -5% to 5%, the band gap of C_2P_4 -1 indicating a linear relationship with the strain ratio, and the band gap of C_2P_4-2 decreases accordingly with different strains. These results indicate that strain is a powerful avenue to modulate their properties, especially the band gap of C_2P_4 -1 can be tuned larger than 2.0 eV which expands their potential applications in optoelectronics.[17] We aslo found that two materials will turn into a metal when the ratio increases to a higher strain ratio.
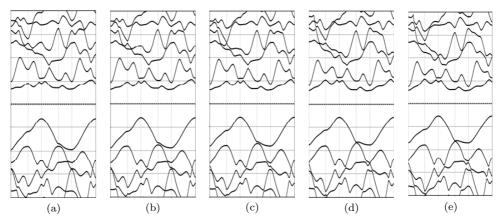
Fig. 12. Band structures of C_2P_4-2 with different uniaxial tensile strain ratios (a) $S_b = 1\%$, (b) $S_b = 2\%$, (c) $S_b = 3\%$, (d) $S_b = 4\%$ and (e) $S_b = 5\%$ along the cell parameter b when stretching the cell parameters.
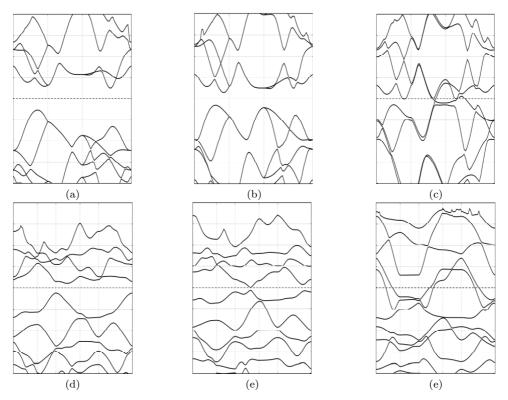

Fig. 13. Band structures of C_2P_4-1 (a)-(c) and C_2P_4-2 (e)-(f) with different larger biaxial tensile strain ratios for the cas of (a) $S_a = -10\%$, (b) $S_a = -15\%$, (c) $S_a = -18\%$ and (a) $S_a = 10\%$, (b) $S_a = 15\%$, (c) $S_a = 20\%$.

Acknowledgements

References

[1] Y. LI, Z. ZHOU, S. ZHANG, Z. CHEN. J. Am. Chem. Soc., (2008), No. 130, 16739–16744.

[2] K. F. MAK, C. LEE, J. HONE, J. SHAN, T. F. HEINZ. Phys. Rev. Lett., (2010), No. 105, 136805.

[3] A. SPLENDIANI, L. SUN, Y. ZHANG, T. LI, J. KIM, C. Y. CHIM, G. GALLI, F. WANG. Nano Lett., (2010), No. 10, 1271–1275.

[4] N. LU, H. Y. GUO, L. LI, J. DAI, L. WANG, W. N. MEI, X. J. WU, X. C. ZENG. *MoS_2/MX_2 heterobilayers: bandgap engineering via tensile strain or external electrical field.* Nanoscale, (2014), No. 6, 2879–2886.

[5] M. T. KUO, P. W. MAY, A. GUNN, M. N. R. ASHFOLD, R. K. WILD. *Studies of phosphorus doped diamond-like carbon films.* Diamond Relat. Mater. (2000), No. 9, 1222.

[6] S. R. J. PEARCE, P. W. MAY, R. K. WILD, A. GUNN, K. R. HALLAM, P. J. HEARD. *Deposition and properties of amorphous carbon phosphide films.* Diamond Relat. Mater (2002), No. 11, 1041.

[7] F. CLAEYSSENS, G. M. FUGE, N. L. ALLAN, P. W. MAY, S. R. J. PEARCE, R. K. WILD, M. N. R. ASHFOLD. *Phosphorus carbide thin films: experiment and theory.* Appl. Phys. A, (2004), No. 79, 1237.

[8] J. N. HART, P. W. MAY, N. L. ALLAN, K. R. HALLAM, F. CLAEYSSENS, G. M. FUGE, M. RUDA, P. J. HEARD. *Towards new binary compounds: Synthesis of amorphous phosphorus carbide by pulsed laser deposition.* J. Sol. State. Chem, (2013), No. 198, 466–474.

[9] W. C. TAN, Y. Q. CAI, R. J. NG, L. HUANG, X. W. FENG, G. ZHANG, Y. W. ZHANG, C. A. NIJHUIS, X. K. LIU, K. W. ANG. *Few-Layer Black Phosphorus Carbide Field-Effect Transistor via Carbon Doping.* Adv. Mater. (2017), No. 29, 1700503.

[10] G. X. WANG, R. PANDEY, S. P. KARNA. *Carbon Phosphide Monolayer with Superior Carrier Mobility.* Nanoscale, (2016), No. 8, 8819–8825.

[11] B. RAJBANSHI, P. SARKAR. *Is the Metallic Phosphorus Carbide (β_0-PC) Monolayer Stable? An Answer from a Theoretical Perspective.* J. Phys. Chem. Lett. (2017), No. 8, 747–754.

[12] G. KRESSE, J. HAFNER. *Ab initio molecular dynamics for liquid metals.* Phys. Rev. B, (1993), No. 47, 558.

[13] G. KRESSE, D. JOUBERT. *From ultrasoft pseudopotentials to the projector augmented-wave method.* Phys. Rev. B, (1999), No. 59, 1758.

[14] J. P. PERDEW, K. BURKE, M. ERNZERHOF. *Generalized Gradient Approximation Made Simple.* Phys. Rev. Lett., (1996), No. 77, 3865.

[15] G. KRESSE, J. FURTHMÜLLER. *Efficient Iterative Schemes for ab-initio Total-Energy Calculations Using a Plane-Wave Basis Set.* Phys. Rev. B, (1996), No. 54, 11169.

[16] G. KRESSE, J. FURTHMÜLLER. *Efficiency of ab-initio Total Energy Calculations for Metals and Semiconductors Using a Plane-Wave Basis Set.* Comput. Mater. Sci. (1996), No. 6, 15–50.

[17] S. L. Zhang, Z. Yan, Y. F. Li, Z. F. Chen, H. B. Zeng. *Atomically Thin Arsenene and Antimonene: Semimetal-Semiconductor and Indirect-Direct Band-Gap Transitions.* Angew. Chem. Int. Ed. (2015), No. 54, 3112–3115.

[18] Y. Zhou, Z. Wang, P. Yang, X. Zu, L. Yang, X. Sun, F. Gao Tensile Strain Switched Ferromagnetism in Layered NbS_2 and $NbSe_2$. ACS Nano, (2012), No. 6, 9727–9736.